LARGE STRAIN LIQUEFACTION TESTS USING MODIFIED HOLLOW CYLINDRICAL TORSIONAL SHEAR APPARATUS

Takashi KIYOTA[1], Takeshi SATO[2] and Junichi KOSEKI[3]

ABSTRACT: In order to study the cyclic behavior of liquefied sands at extremely large strain levels up to double amplitude shear strain of about 100 %, a series of undrained cyclic torsional shear tests was performed on saturated Toyoura sand under different densities, two kinds of in-situ frozen sandy samples and their reconstituted specimens. After exceeding a certain level of overall shear strain, localization of specimen deformation was observed. The initiation of such localization was associated with the changes in the cyclic amplitude of deviator stress and the increment of shear strain. In the case of Toyoura sand, the limiting value of shear strain to initiate strain localization was found to increase with decrease in the relative density. In the case of in-situ frozen sandy samples, their limiting shear strain values were smaller than those of the reconstituted specimens, suggesting that their soil structures were different from each other under different degrees of natural aging effects.

Key Words: Liquefaction, Sand, In-situ frozen sample, Large strain, Torsional shear

INTRODUCTION

Occasionally, extremely large deformation could be observed on liquefied soil. For example, during the 1964 Niigata and 1983 Nihonkai-Chubu earthquakes, liquefaction-induced ground displacement reached several meters (Hamada et al., 1993). It was also the case with reclaimed ground behind quay walls during the 1995 Hyogoken-Nanbu earthquake (Ishihara et al., 1996). These large displacements are associated with strains that are induced in the liquefied ground on the order of several tens of percent or even larger, as have been observed in relevant model tests (e.g., Yasuda et al., 1992 among others).

Large deformation of liquefied soils has been also observed in model tests near underground structures that are uplifted due to liquefaction of surrounding soils (Koseki et al., 1997). However, it is not an easy task to simulate large deformation of liquefied soils in laboratory element tests. In conventional triaxial tests, for example, the axial strain levels employed are usually limited to 20 % or less, due to larger extents of non-uniform deformation of the specimen at higher strain levels.

In contrast, in torsional shear tests on hollow cylindrical specimens, one can achieve higher strain levels by increasing the amount of torsional displacement that is applied to the specimen through rotating the top cap. For example, Yasuda et al. (1995) investigated into the properties of liquefied sands under undrained monotonic torsional shear loading up to shear strain levels of about 50 %. However, as far as the authors know, there has been no study on cyclic behavior of liquefied sands up to such large strain levels, due possibly to the technical difficulties in correcting for the effects of

---

[1] Assistant Professor, Tokyo University of Science
[2] Research Support Promotion Member
[3] Professor

membrane force during the tests.

In view of the above, in the present study, in order to study the cyclic behavior of sands during the process of liquefaction up to extremely large strain levels, a series of undrained cyclic torsional shear tests was performed on three kinds of sandy soils up to double amplitude shear strain of about 100 %, while correcting for the effects of membrane force on the measured shear stress during the test.

TEST APPARATUS

The test apparatus used in this study is shown in Fig. 1. In order to enlarge the effective range of torsional displacement, an improvement was made on the one employed by HongNam and Koseki (2005) by modifying the belt-driven torsional loading system that is connected to an AC servo motor through electro-magnetic clutches and reduction gears (Fig. 1b). The details of the torque-transmission part after modification are shown in Fig. 1c). The linear-motion guide has a stroke of 60 cm, which can rotate the loading shaft by about 1.2 rounds through a pulley having a diameter of 15 cm.

From the above modifications, it was made possible to achieve double amplitude torsional shear strain levels exceeding 100 %. In order to evaluate such large torsional deformation, as shown in Figs. 1b) and c), a potentiometer with a wire and a pulley was employed. Torque and vertical load were measured with a two-component load cell that is installed inside the pressure cell (Fig. 1a)).

This loading device is a displacement-controlled type from a mechanical point of view, whereas cyclic shear tests by keeping the specified shear stress amplitude τ_d could be conducted by using a computer which monitors the outputs from the load cell and controls the device accordingly. Refer to Koseki et al. (2005) for the details of the stress computations.
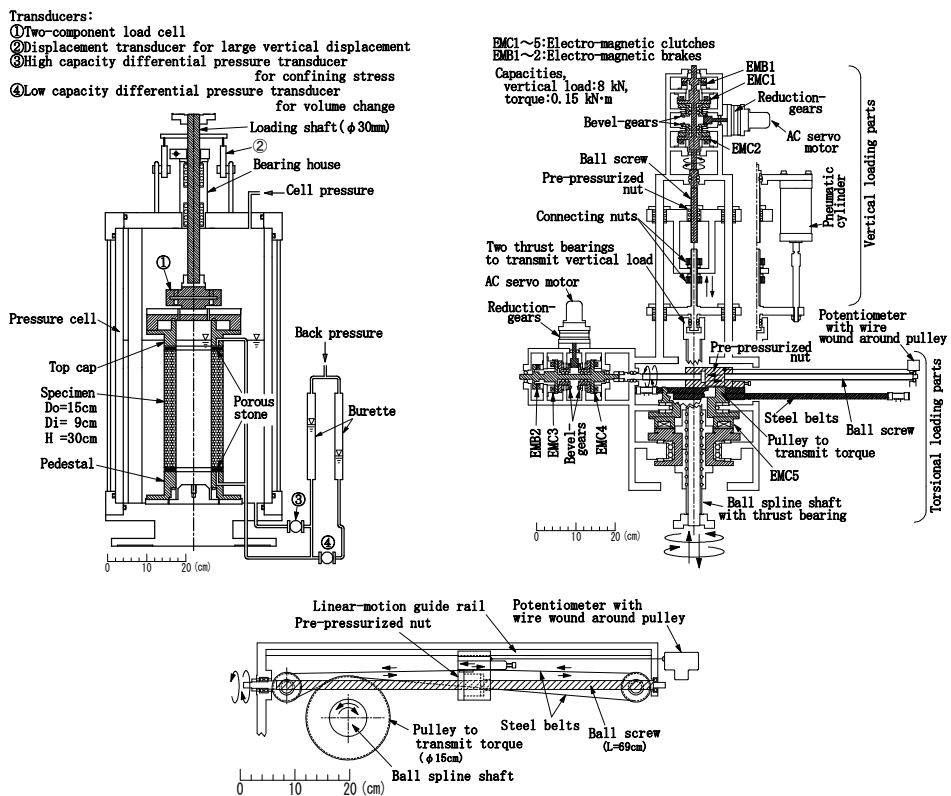

Figure 1   a) Torsional shear test apparatus on hollow cylindrical specimen, b) loading device and c) plan view of toruque-transmission part.

TEST PROCEDURE

In this study, three kinds of materials as shown in Table 1 were employed. One of the test materials was Toyoura sand, a uniform sand with sub-angular particles. The specimens were prepared by pluviating air-dried sand particles through air. In total, 12 specimens with different values of initial relative density in the range of approximately 15 to 90 % were prepared by changing the height of pluviation. After saturating the specimens with pouring carbon dioxide through the void among the sand particles and then pouring de-aired water, they were consolidated to an isotropic effective stress state of 100 kPa with a back pressure of 200 kPa.

The other test materials were Edo-river B sand and Edo-river C sand, which were taken by in-situ freezing sampling technique from Pleistocene deposits. Thawing the in-situ frozen samples (FSs) at a lower confining pressure might be one of the possible factors to cause sample disturbance (Kiyota et al., 2006). In this study, therefore, a confining pressure of 98 kPa was applied during thawing by a vacuum pump. It is equivalent to the in-situ overburden stress at the depth of sampling of Edo-river B sand as well as the limit value of the capacity of conventional vacuum pumps. After saturating the specimens with keeping the confining pressure at 98 kPa, they were consolidated to an isotropic effective stress state of 100 kPa with Edo-river B sand and that of 160 kPa with Edo-river C sand with a back pressure of 200 kPa. These isotropic stresses will be denoted as σ_m' herein.

Table 1 Material properties

Specimens	Sampling depth (GL- m)	Specific gravity, G_s	Maximum void ratio, e_{max}	Minimum void ratio, e_{min}	Mean diameter, D_{50} (mm)	Fines content, F_c (%)
Toyoura sand	-	2.635	0.975	0.561	0.20	0.1
Edo-river B sand	10	2.859	1.043	0.710	0.56	3.0
Edo-river C sand	16	2.758	1.765	1.052	0.15	9.0

The reconstituted samples (RSs) of Edo-river B and C sands were prepared in a specimen mold with adjusting the dry density by tapping the mold to the same level as that of respective FS. After saturating the specimens at a confining pressure of 30 kPa, they were consolidated to the same isotropic effective stress states as those of respective FSs with a back pressure of 200 kPa. After isotropic consolidation, some of the RSs were subjected to 20,000 cycles of torsional load with double amplitude shear strain, $\gamma_{(DA)}$, of approximately 0.2 % under drained condition. This is one of the procedures to increase the liquefaction strength without significantly changing the specimen density (e.g., Seed, 1979), and the RS which has such a stress history is called RSCL in this paper.

After the above procedures, undrained cyclic torsional tests were performed on FSs, RSs and RSCLs. Using the modified loading device, the torsional torque was applied at a constant shear strain rate of 5.5 %/min. The loading direction was reversed when the shear stress amplitude, τ_d, that was corrected for the effects of membrane force reached the specified value. Throughout the cyclic torsional loading, the vertical strain of the specimen was maintained to be zero, by using a mechanical locking device for the vertical displacement of the top cap.

TEST RESULTS AND DISCUSSION

Correction for membrane force
Usually, the membrane force has been corrected based on the elasticity theory which employs the Young's modulus of the membrane. Therefore, first, to confirm the applicability of the theoretical value to the apparent shear stress, τ_m, that is mobilized by the membrane due to torsional deformation up to double amplitude shear strain, $\gamma_{(DA)}$, of about 100 %, it was compared with the actual membrane

force that was measured by filling water between the outer and inner membranes and shearing it under undrained condition. The theoretical value in terms of the apparent shear stress, τ_m, of the outer and inner membranes due to torsional deformation was evaluated as:

$$\tau_m = \frac{t_m E_m \left(r_o^3 + r_i^3\right)\theta}{\left(r_o^3 + r_i^3\right)h} \tag{1}$$

where θ is rotational angle of the top cap measured with a potentiometer (Figs. 1b) and c)); h is the height of the specimen; r_o and r_i are the outer and the inner radii of the specimen; and t_m and E_m are the thickness (= 0.3 mm) and Young's modulus (=1492 kPa), respectively, of the membrane.

Figure 2 shows the relationships between shear stress and shear strain of the membrane obtained theoretically and experimentally. The difference in the deformation modes of the membranes that were assumed in the theory and mobilized in reality became larger as $\gamma_{(DA)}$ was increased, and then some discrepancy was observed between them under larger strain levels at $\gamma_{(DA)}= 100$ %. Therefore, the measured τ_m-γ relation that is approximated by the polynomial as shown in Fig. 2 is employed for the correction of membrane force later.
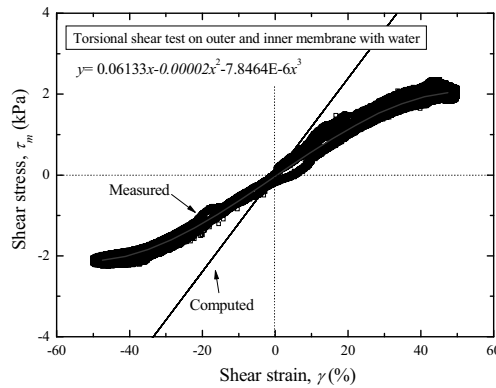

Figure 2   Relationships between apparent shear stress due to membrane force and shear strain

Toyoura sand

Typical test results on relatively loose and medium loose specimens of Toyoura sand are shown in Figs. 3 and 4, respectively. The cyclic mobility was observed in Figs. 3a) and 4a) where the effective stress was recovered repeatedly after showing zero effective stress state. It was accompanied with a significant development of double amplitude shear strain, $\gamma_{(DA)}$, as shown in Figs. 3b) and 4b). The shear strain that was induced at the time intervals when the effective stress became almost zero increased with the increase in the number of cycles. This behaviour is known as a typical result of liquefaction tests on clean sand, and has been reported by previous studies (e. g., Shamoto et al., 1997).

The specimen deformation at several states as numbered 1 through 4 in Fig. 3 is shown in Photo 1. At state 1 with a shear strain, γ, of about 15 %, the deformation was rather uniform except for the regions near the top cap and the pedestal that are affected by the end restraint. At state 2 with the γ value of about -35 %, the outer membrane wrinkled at several locations. It seems that the deformation of the specimen started to localize, in particular in the upper part of the specimen. At state 3 with the γ value of about 50 %, the localization of the specimen deformation developed with increase in strain level in the upper part of the specimen. At state 4 with the γ value of about -65 %, the specimen was twisted extensively.
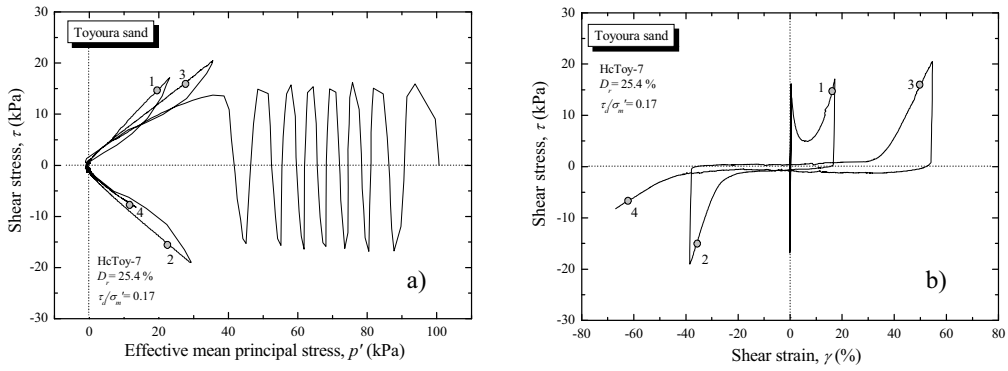
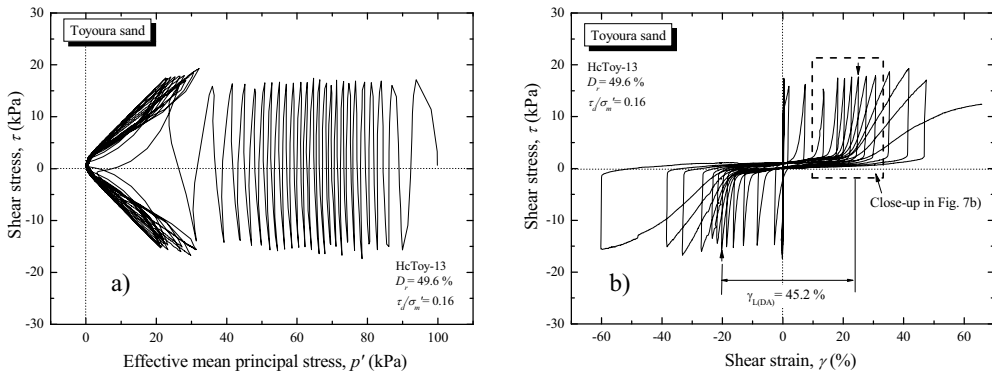Figure 3   Typical test result on loose Toyoura sand (Dr= 25.4 %)

Figure 4   Typical test result on medium loose Toyoura sand (Dr= 49.6 %)

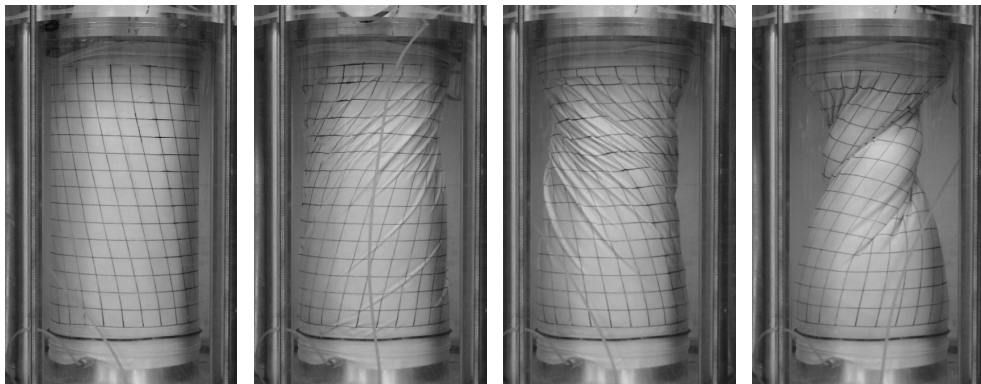| a) State 1	b) State 2	c) State 3	d) State 4
(γ= 15 %)	(γ= -35 %)	(γ= 50 %)	(γ= -65 %)

Photo 1   Specimen deformation at states 1 through 4 shown in Fig. 3 (Toyoura sand)

In the case of conventional triaxial tests, strain levels employed are usually limited to several percent to about 20 %. In the present study, on the other hand, using the torque loading device that was modified for enlarging the effective range of torsional displacement, the liquefaction characteristics of the shear strain levels on the order of several tens of percent or even larger could be obtained.

In the present tests, the $\gamma_{(DA)}$ values continued to increase and approached 100 % that is the capacity

of the apparatus, irrespective of specimen densities. However, non-uniform deformation or strain localization was observed at higher strain levels as shown in Photo 1c).

Since the initiation of strain localization could not be clearly defined based on the visual observation of the specimen deformation, it was defined based on the change in the response of the deviator stress, q. For example, after passing state A shown in Fig. 5a), the amplitude of the cyclic change in the deviator stress decreased suddenly. It was accompanied with an increase in the increment of single amplitude shear strain, $\Delta\gamma$, and double amplitude shear strain, $\gamma_{(DA)}$, as shown in Figs. 5b). It should be noted that, before reaching state A, the value of $\Delta\gamma$ and $\Delta\gamma_{(DA)}$ decreased with an increase in the number of cycles. Therefore, such state A was considered in the present study as the limiting state to initiate strain localization, and thus the limiting value of double amplitude shear strain, $\gamma_{L(DA)}$, to initiate strain localization was defined based on the last cycle data when the limiting state appeared.

As a result, the $\gamma_{L(DA)}$ value was found to increase with a decrease in the relative density of the specimen, as shown in Fig. 6. In addition, it seems that the values of $\gamma_{L(DA)}$ were independent from the values of shear stress ratio, τ_d/σ'_m, during undrained cyclic loading.

It should be noted that, as indicated by a horizontal arrow in Fig. 6, in the case of loose specimens with a relative density of less than 30 %, the values of $\gamma_{L(DA)}$ may have been underestimated. With these specimens, as typically shown in Fig. 3, the increment in the shear strain amplitude increased suddenly during the tests. One may expect that, if the increment in the shear strain amplitude had been much smaller, then the above limiting state might have been observed again. Therefore, it would in general result in underestimation of the $\gamma_{L(DA)}$ values with loose specimens to evaluate them following the above definition based on the last cycle data that exhibited the limiting state.
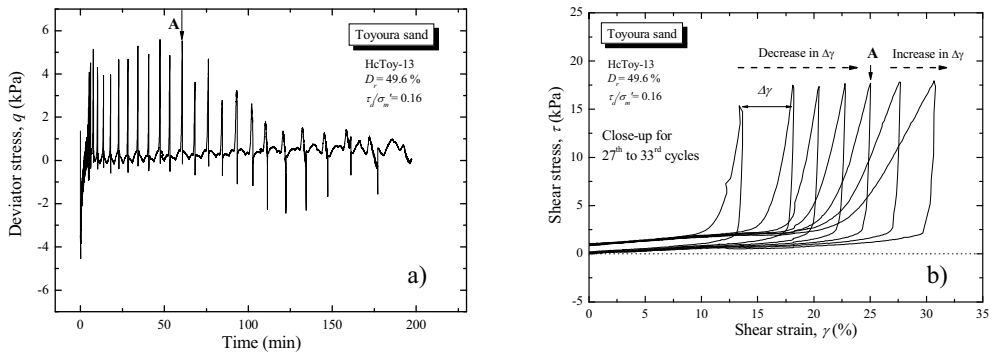

Figure 5 a) Time history of deviator stress, b) Change in shear strain during cyclic loading (cf. Fig. 4)
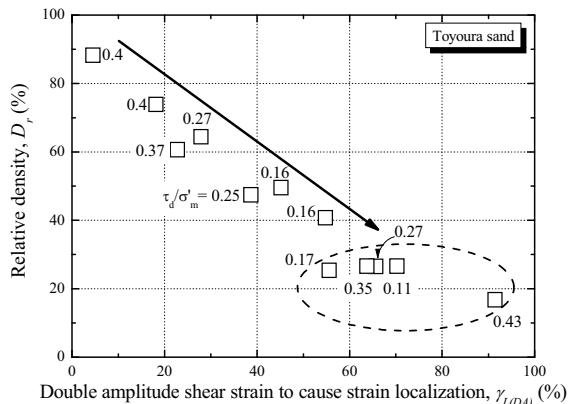

Figure 6   Relationship between limiting value of shear strain and relative density of Toyoura sand

In-situ frozen sandy samples and their reconstituted specimens

A typical test result on FS of Edo-river B sand is shown in Fig. 7. The cyclic mobility was observed, and the double amplitude shear strain, $\gamma_{(DA)}$, caused by undrained cyclic loading exceeded 90 %. The general trend of the γ–τ relation of this FS seems to be similar to that of medium loose or medium dense Toyoura sand, where shear strains developed gradually with the increase in number of cycles (Fig. 4).

The specimen deformation at several states as numbered 1 through 4 in Fig. 7 is shown in Photo 2. At state 1 with a shear strain, γ, of about -5 %, the deformation was rather uniform. At state 2 with the γ value of about -14 %, the localized deformation was initiated in the upper part of the specimen. At state 3 with the γ value of about 20 %, the specimen deformation was further localized in a zone beneath the top cap. At state 4 with the γ value of about 45 %, the deformation in the above zone of the specimen was localized significantly, while those of the middle and bottom parts of the specimen were relatively small.
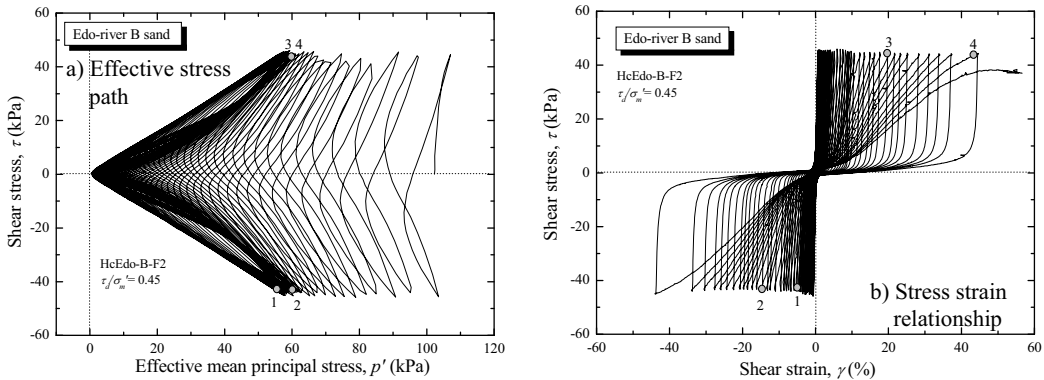

Figure 7   Typical test result on FS of Edo-river B sand (Dr= 74.5 %)

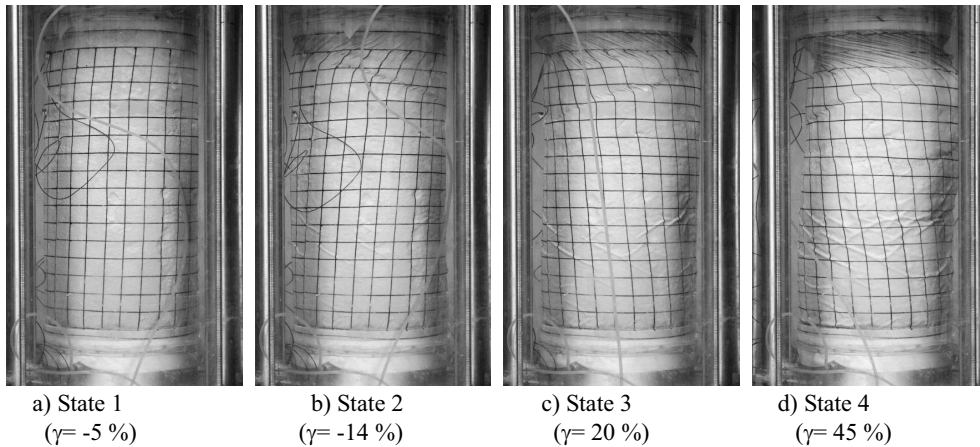| a) State 1 | b) State 2 | c) State 3 | d) State 4 |
| (γ= -5 %) | (γ= -14 %) | (γ= 20 %) | (γ= 45 %) |

Photo 2   Specimen deformation at states 1 through 4 shown in Fig. 9 (Edo-river B sand, FS)

Figures 8a) and b) show test results of RS and RSCL of Edo-river B sand. Although the relative density of the RS was somewhat higher than that of the FS (Fig. 7), the RS was more vulnerable to liquefaction than the FS. For example, as shown in Fig. 8a), the effective stress of the RS was

decreased significantly at the first cycle, whereas that of the FS was decreased gradually with the increase in the number of cycles as shown in Fig. 7a). This discrepancy may be explained by assuming that the FSs would have a natural aging effect which causes soil structure to be strengthened with inter-locking or cementation between the soil particles, while the RSs wouldn't have any such effect. Similar test results that liquefaction resistance of the FS is larger than that of the RS have been reported by Yoshimi et al. (1984) and Hatanaka et al., (1988). On the other hand, the extent of the reduction of effective stress of the RSCL was much smaller than that of the RS. The higher liquefaction resistance of the RSCL was caused possibly by formation of inter-locking of the soil particle due to the application of drained cyclic loading before the liquefaction test. Rather, although the relative density of the RSCL was somewhat higher than that of the FS (Fig. 7), the liquefaction behaviour of the RSCL corresponded well to that of the FS.

Another series of experiments were performed with Edo-river C sand. As shown in Figs. 9a) and b), the change in the reduction rate of effective stress during cyclic loading between the FS and the RS of Edo-river C sand were similar to that of Edo-river B sand shown in Figs. 7a) and 8a). In addition, as shown in Figs. 9b) and c), the liquefaction resistance of the RSCL of Edo-river C sand was larger than that of the RS.

However, as can be seen from Figs. 9a) and c), the liquefaction resistance of the RSCL was still lower than that of the FS for Edo-river C sand, while they were rather similar to each other for Edo-river B sand (Figs. 7a) and 8b)). This feature may suggest that the aging effect of the FS of Edo-river C sand was stronger than that of Edo-river B sand because the geological age of Edo-river C sand is older than that of Edo-river B sand based on their sampling depths as shown in Table 1.
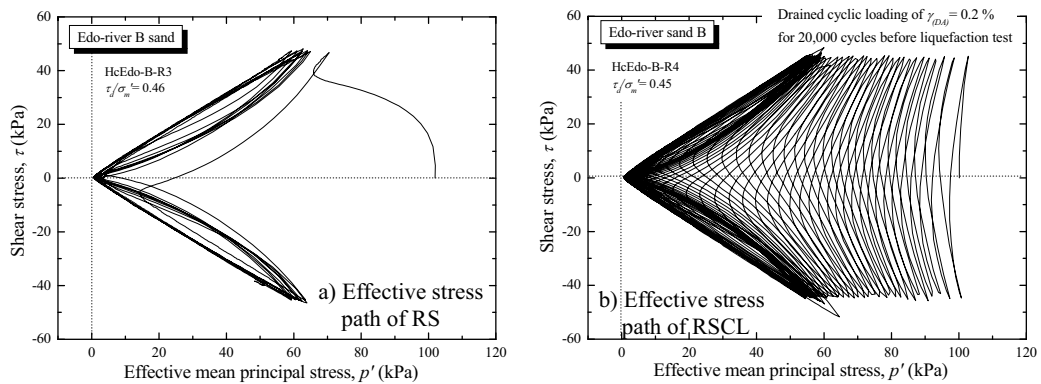

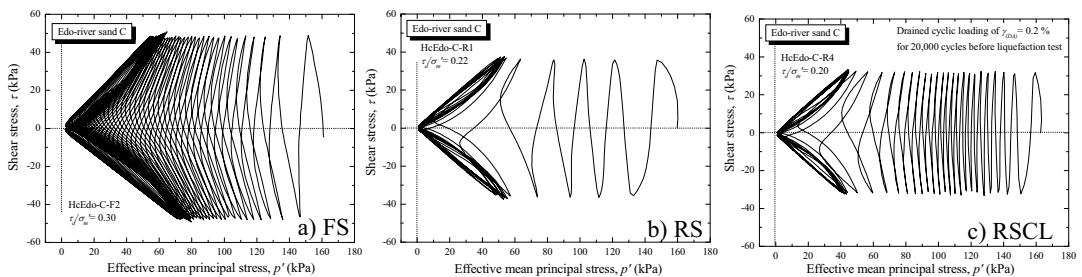Figure 8   Typical test result on a) RS (Dr= 89.7 %) and b) RSCL (Dr= 97.2 %) of Edo-river B sand

Figure 9   Effective stress paths of Edo-river C sand

The limiting value of double amplitude shear strain, $\gamma_{L(DA)}$, to initiate strain localization was also investigated with FSs, RSs and RSCLs of Edo-river B and C sands. Figure 10 shows the relationship between $\gamma_{L(DA)}$ and the relative density of these samples. In addition, the test results of Toyoura sand as mentioned above are also plotted in Fig. 10.

As mentioned previously, the values of $\gamma_{L(DA)}$ of Toyoura sand increased with the decrease in the relative density of the specimen. On the other hand, the $\gamma_{L(DA)}$ values of the FSs of Edo-river B and C sands were significantly smaller than those of the RSs and the RSCLs even though the relative densities of the FSs were somewhat lower than those of the RSs or the RSCLs. In addition, smaller values of $\gamma_{L(DA)}$ were observed with the RSCLs in comparison with those of the RSs for both Edo-river B and C sands.

Although the value of $\gamma_{L(DA)}$ of Toyoura sand was correlated well with relative density of the specimen, there was no corresponding change in the $\gamma_{L(DA)}$ with the relative density of the specimens for the FSs, RSs and RSCLs despite using the same material. Such discrepancy reflects possibly the difference in soil structure of the specimens. In the case of Toyoura sand, the soil structures of the specimen might be similar to each other because all specimens were prepared by the same method. Therefore, the values of $\gamma_{L(DA)}$ depended predominantly on the relative density of the specimen. However, in the case of reconstituted samples, the soil structures of the RSCLs would change from those of the RSs due to the application of drained cyclic loading before liquefaction tests.

In addition, the soil structure of the FSs which were retrieved in-situ would be more complicated than those of the reconstituted samples, because the FSs would have inherent soil structure which are affected by natural environments; for example, creep loading with time, earthquake histories, change in the overburden pressure due to change in the water table or the land form. Therefore, the values of $\gamma_{L(DA)}$ would not depend only on the relative density of the specimens for the FSs, RSs and RSCLs. Moreover, in the case of Pleistocene deposit like the FSs employed in this study, cementation effect may have also taken place due to the chemical reaction as time passed by. Consequently, the soil structure of the FSs would be more stabilized than those of the RSs and the RSCLs which would have no cementation effect, and thus the $\gamma_{L(DA)}$ values of the FSs were smaller than those of the RSs and the RSCLs.
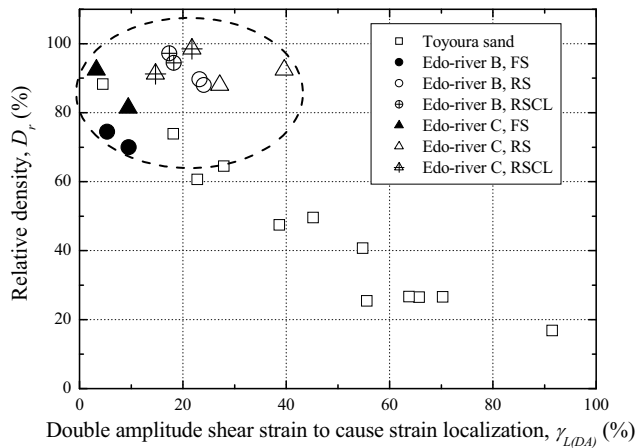

Figure 10   Relationship between limiting value of overall shear strain and relative density of in-situ samples

CONCLUSIONS

A series of undrained cyclic torsional shear tests was conducted on Toyoura sand and two kinds of in-situ frozen sandy samples and their reconstituted specimens, in which the specimen height was kept constant during shearing. The test results could be summarized as follows;

a) Undrained cyclic torsional shear tests could be performed up to double amplitude shear strain of approximately 100 % by using the modified torque loading device for enlarging the range of torsional displacement.

b) By correcting for the effect of membrane force on the measured shear stress, reasonable stress strain relationships and liquefaction resistance curves which reflect liquefaction characteristics of the specimen with different densities could be obtained even under large strain levels.

c) Localization of specimen deformation was observed during the tests, and initiation of such strain localization was associated with the change in the cyclic amplitude of deviator stress and the increment of shear strain. It was associated with the initiation of strain softening behaviour that was observed in the relationships between the modified shear stress ratio and shear strain.

d) In the case of Toyoura sand, the limiting value of double amplitude shear strain, $\gamma_{L(DA)}$, to initiate strain localization was found to increase with a decrease in the relative density of the specimen. In the case of in-situ frozen sandy samples, their $\gamma_{L(DA)}$ values were smaller than those of the reconstituted specimens. Such discrepancy reflects possibly the difference in soil structures that has been caused by different degrees of natural aging effects.

REFERENCES

Hamada, M., O'Rourke, T.D. and Yoshida, N. (1993): Liquefaction-induced large ground displacement, *Performance of Ground and Soil Structures during Earthquakes, 13th ICSMFE, JGS*, 93-108.

Hatanaka, M., Suzuki, Y., Kawasaki, T. And Endo, M. (1988): Cyclic undrained shear properties of high quality undisturbed Tokyo gravel, *Soils and Foundations*, **28** (4), 57-68.

HongNam, N. and Koseki, J. (2005): Quasi-elastic deformation properties of Toyoura sand in cyclic triaxial and torsional loadings, *Soils and Foundations*, **45**(5), 19-38.

Ishihara, K., Yasuda, S. and Nagase, H. (1996): Soil characteristics and ground damage, *Soils and Foundations, Special Issue on Geotechnical Aspects of the January 17 1995 Hyogoken-Nambu Earthquake*, 109-118.

Kiyota, T., Sato, T., Koseki, J. and Tsutsumi, Y. (2006): Comparison of liquefaction properties of in-situ frozen and reconstituted sandy soils, *Proc. of the International Symposium on Geomechanics and Geotechnics of Particulate Media* (Hyodo et al. eds), 113-119.

Koseki, J., Matsuo, O. and Koga Y. (1997): Uplift behavior of underground structures caused by liquefaction of surrounding soil during earthquake, *Soils and Foundations*, **37**(1), 97-108.

Koseki, J., Yoshida, T. and Sato, T. (2005): Liquefaction properties of Toyoura sand in cyclic torsional shear tests under low confining stress, *Soils and Foundations*, **45**(5), 103-113.

Seed, H.B. (1979): Soil liquefaction and cyclic mobility evaluation for level ground during earthquakes, *Journal of the Geotechnical Engineering Division*, ASCE, Vol. 105, No. GT2, 201-255.

Shamoto, Y., Zhang, J.-M. and Goto, S. (1997): Mechanism of large post-liquefaction deformation in saturated sand, *Soils and Foundations*, **38**(2), 71-80.

Yasuda, S., Nagase, H., Kiku, H. and Uchida, Y. (1992): The mechanism and a simplified procedure for the analysis of permanent ground displacement due to liquefaction, *Soils and Foundations*, **32**(1), 149-160.

Yasuda, S., Yoshida, N., Masuda, T., Nagase, H., Mine, K. and Kiku, H. (1995): Stress-strain relationships of liquefied sands, *Earthquake Geotechnical Engineering*, Ishihara (ed.), **2**, 811-816.

Yoshimi, Y., Tokimatsu, K., Kaneko, O. and Makihara, Y. (1984): Undrained cyclic shear strength of a dense Niigata sand, *Soils and Foundations*, **24** (4), 131-145.